Submillimeter-Wavelength Plasma Diagnostics For Semiconductor Manufacturing

Eric C. Benck[1], Guerman Yu. Golubiatnikov[1], Gerald T. Fraser[1], David Pluesquelic[1],

Rich Lavrich[1], Bing Ji[2], Stephen A. Motika[2], and Eugene J. Karwacki[2]

[1]National Institute of Standards and Technology, Gaithersburg, MD 20899
[2]Air Products and Chemicals, Inc., Allentown, PA 18195

Abstract. Submillimeter-wavelength, linear-absorption spectroscopy has been applied as a chemical diagnostic of a reactive-ion etching plasma in a modified capacitively coupled Gaseous Electronics Conference (GEC) reactor. Approximately 1 mW of narrow-band (< 10 kHz) submillimeter radiation between 450 GHz and 750 GHz is produced using a backward-wave oscillator (BWO). The submillimeter method offers high sensitivity for the $\approx$ 1 MHz linewidth, Doppler-broadened absorption lines typical of gas-phase molecules at a total pressure of less than 133 Pa (1 Torr). A large variety of molecules can be detected, limited primarily by the need for a permanent electric dipole moment and for accurate line frequency predictions, which are often available in the literature. The capabilities of the diagnostic method have been demonstrated by the following three applications: 1) the measurement of water-vapor contamination in the reactor and in the precursor gas; 2) the assessment of progress in the cleaning of the reactor; and 3) the determination of the endpoint in the etching of a SiO_2 thin film on silicon.

INTRODUCTION

Progress in plasma processing for semiconductor manufacturing is becoming increasingly dependent on *in situ* diagnostics, i.e., on the ability to quantitatively and nonintrusively measure physical and chemical properties of the plasma, such as electron and molecular temperatures and concentrations and their spatial distributions. The information obtained from such measurements aids the advancement and validation of sophisticated computational plasma models. These models are required to respond to industry demands for better plasma processing technology for semiconductor manufacturing. The technology needs include ensuring good etch uniformity over increasingly larger wafer surface areas, being able to produce smaller, more sophisticated, and higher aspect-ratio features, reducing chamber cleaning time and frequency, decreasing the consumption of expensive process gases, and eliminating toxic, atmospheric greenhouse contributing, and stratospheric-ozone-depleting effluent emissions.

Submillimeter-wavelength absorption spectroscopy has the potential of being an important *in situ* plasma diagnostic. Radiation in this frequency range (300 GHz to 1000 GHz) couples to the rotational energy levels of most molecules. Essentially any noncentrosymmetric molecule with a permanent electric dipole moment will have a strong absorption in this spectral region. Consequently, most of the important plasma radicals can be monitored with submillimeter-wavelength radiation.

EXPERIMENTAL APPARATUS

Chemical-diagnostic measurements on a model reactor for plasma etching were performed using a submillimeter-wavelength linear-absorption spectrometer which is similar to the instrument described by Krupnov and Pavlovsky.[1, 2] The submillimeter source is a 450 GHz to 750 GHz commercial backward-wave-oscillator (BWO) electronic tube. This continuous wave (cw) electron tube device acts

as a voltage controlled frequency source. It is operated in a magnetic field of approximately 11 kG, produced between the poles of a pair of NdFeB permanent magnets. The tube generates approximately 1 mW of output with a linewidth of <10 kHz. It can be referenced to an atomic clock or crystal oscillator for exceptional frequency metrology.

The submillimeter-wavelength radiation is detected with a liquid helium cooled bolometer. Second harmonic frequency modulation is used to improve the signal-to-noise ratio of the measurements. In order to calibrate the detector sensitivity, calibration measurements are made without a plasma using a stable gas at a known density. For these measurements, COF_2 was the calibration gas.

The plasma source was a modified capacitively coupled Gaseous Electronics Conference (GEC) Reference Source.[3, 4] This plasma source was designed to create plasmas similar to those found in commercial etching reactors, but while allowing ample access for plasma diagnostics. This particular source was modified from the original GEC design by replacing the powered electrode with a commercial electrostatic chuck with helium backside cooling and increasing the diameter of the grounded electrode.

RESULTS

Below we illustrate three applications of the submillimeter chemical diagnostics technique.

Measurement of Water-Vapor Contamination

Water-vapor contamination is of concern in many semiconductor manufacturing processes[5]. Submillimeter spectroscopy enables the direct and sensitive measurement of water-vapor contamination in the plasma reactor prior to initiation of the plasma, using the intense $1_{10} - 1_{01}$ absorption line at ν = 556.936 GHz. The measurement of water contamination is optimally performed without the plasma to minimize water-vapor decomposition and thus enhance detection sensitivity. We further note that the amount of water-vapor contamination, as judged by the strength of this water vapor submillimeter transition, dropped below our sensitivity level
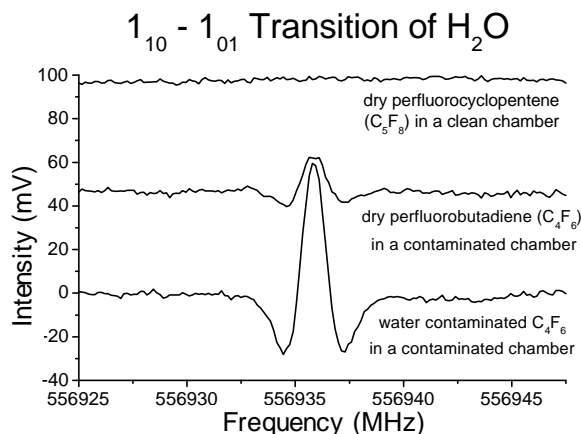

FIGURE 1. Spectra of the $1_{10} - 1_{01}$ rotational transition of water vapor in the reactor with the plasma off in three different 6.6 Pa (50 mTorr) samples to assess water-vapor contamination from the reactor and the feed-gas stream. The spectra correspond to approximately 30 s of signal averaging. The sample for the top trace (a) was obtained from a flow of 14.3 sccm (1 sccm = .745 μmol/s) of octafluorocyclopentene (C_5F_8), 77.1 sccm of Ar, and 18.6 sccm of O_2 and revealed a water-vapor contamination of $< 8 \times 10^7$ cm^{-3}. The samples from the middle (b) and bottom (c) traces were obtained from a flow of 14.3 sccm hexafluoro-1,3-butadiene (C_4F_6), 74.2 sccm of Ar, and 21.5 sccm O_2. The source of the 4.6×10^8 cm^{-3} water-vapor impurity in the middle chamber is a contaminated chamber while the sources of the 1.9×10^9 cm^{-3} water-vapor impurity in the lower trace are both a contaminated C_4F_6 sample and chamber.

whenever the plasma was ignited, for a range of initial contamination levels of interest.

Monitoring the gas in the reactor allows the quantification of total water-vapor contamination, i.e. that coming from the original feed gas, the transport lines to the reactor, and from outgassing of the reactor walls. Performing the measurements just after the chamber cleaning step ensures that the chamber components are at an elevated temperature necessary to produce a water-vapor outgassing level similar to that expected during etching.

In Fig. 1 we show the recorded water-vapor spectra for three 6.6 Pa (50 mTorr) samples in the reactor vessel. The top octafluorocyclopentene (C_5F_8) sample shows no water-vapor contamination at our level of sensitivity of approximately 0.32 μPa (2.4×10^{-6} mTorr) for a 39 cm pathlength through the reactor. The middle high-purity hexafluoro-1,3-butadiene (C_4F_6) sample shows a trace level of water-vapor contamination of 4.6×10^8 cm^{-3}, while the bottom lower-purity
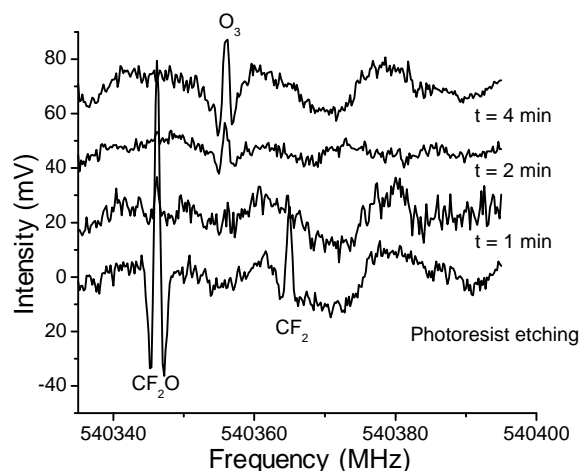
FIGURE 2. Spectra as a function of time during the cleaning of a plasma reactor after the etching of a photoresist-coated Si wafer using a plasma formed by flowing Ar, O_2, and C_5F_8 at 77.1 sccm, 18.6 sccm, and 14.3 sccm, respectively, and at a total pressure of 50 mTorr. The bottom trace was recorded while the photoresist was being etched and shows an unassigned CF_2O line, also observed under plasma-free conditions in a $CF_2O:N_2$ mixture, and the $18_{2,17}$ - $17_{1,16}$ line of CF_2. The average chamber densities of CF_2O and CF_2 derived from the intensities of these lines are 1.0×10^{13} cm^{-3} and 4.7×10^{11} cm^{-3}, respectively, for the bottom trace. Then the chamber was cleaned with a 50 mTorr Ar/O_2 plasma using Ar and O_2 flow rates of 50 sccm each. The CF_2O and CF_2 transitions rapidly disappear during the chamber cleaning (1 min, 2 min, and 4 min traces), and indeed have effectively vanished after approximately 2 min (2 min trace) into the process. Concomitant with the reduction of these fluorocarbon transitions, the O_3 transition ($11_{5,7}$ - $12_{4,8}$) increases in intensity to a level corresponding to a concentration of O_3 of 1.3×10^{12} cm^{-3} after 4 min, as shown in the top trace.

hexafluoro-1,3-butadiene (C_4F_6) sample trace shows the highest level of water-vapor contamination, 1.9×10^9 cm^{-3}, approximately 3 times greater than the middle trace based on the ratio of the peak intensities. The spectra were recorded by twice sweeping the submillimeter frequency across the absorption feature using a time constant of 30 ms and a total scan time from 30 to 40 s, and then averaging the two traces. The acquisition time of the system could be reduced by a factor of three by minimizing the capture of baseline data points outside of the line profile. Further reduction in the acquisition time to < 0.5 s could be achieved without significantly reducing sensitivity by capturing just two data points: one at the line center and one outside of the line profile to provide a baseline reference. The absolute sensitivity level obtained for water vapor of 0.32 μPa (2.4 nTorr)(7.7×10^7 cm^{-3}) in the reactor corresponds to a fractional molar concentration of
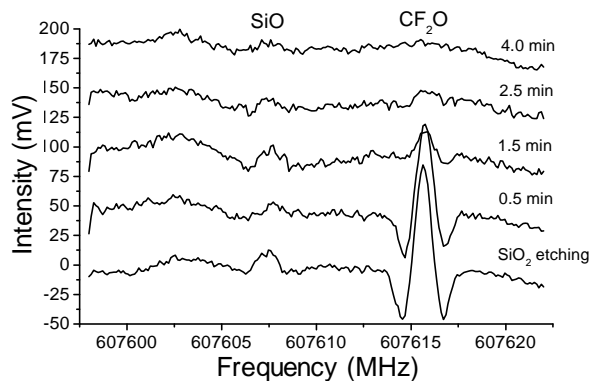

FIGURE 3. Spectra observed for an Ar/O_2 cleaning plasma (50 sccm Ar and 50 sccm O_2 at a chamber pressure of 6.7 Pa) following the etching of a SiO_2 layer on a Si wafer by a fluorocarbon plasma (14.3 sccm C_5F_8, 18.6 sccm O_2, and 77.1 sccm Ar at a chamber pressure of 6.7 Pa). The bottom trace shows a spectrum during the etching of the wafer, while the top four traces show spectra recorded from 0.5 min to 4.0 min into the cleaning process. The average number density obtained for SiO ($J = 14$ - 13 transition) and CF_2O (unassigned transition) from the bottom trace are 5.7×10^7 cm^{-3} and 2.0×10^{13} cm^{-3}, respectively.

2.4 nmol/mol (2.4 ppb) for a hypothetical 133 Pa (1 Torr) sample. This level of sensitivity could be improved by signal averaging, multipassing the submillimeter beam through the reactor using a multipass cell or a resonant cavity to increase ℓ, or reducing amplitude noise on the submillimeter radiation. A sensitivity level of 0.5 nmol/mol or 0.5 ppb should be easily achievable, and we eventually expect that levels as small as 0.1 nmol/mol or 0.1 ppb will be possible. At these levels of sensitivity, submillimeter spectroscopy would challenge other water-vapor optical sensors presently in use or under development in simplicity, sensitivity, and cost.

Assessment of Chamber Cleaning Progress

To ensure the reproducibility of the multiple plasma processing steps in semiconductor wafer fabrication it is generally desired to clean the reactor chamber at selected intervals during the process. In the present set of investigations, after a wafer was etched it was replaced by a bare silicon wafer and the chamber cleaned by running an equimolar 6.7 Pa (50 mTorr) Ar/O_2 plasma for 4 minutes, with each gas flowing at 50 standard cubic cm per minute (sccm). To assess the performance and better understand the complex chemistry of the cleaning process, submillimeter measurements were made of CF_2O,

CF$_2$, SiO, and O$_3$ transitions in the reactor as a function of time after initiation of the cleaning step. Figures 2 and 3 show some of the results of this study. In both figures, a reference trace is presented at the bottom showing either the etching of a photoresist (Fig. 2) or of SiO$_2$ on Si (Fig. 3) both using a 6.7 Pa (50 mTorr) mixture of Ar, O$_2$, and C$_5$F$_8$ (perfluorocyclopentene) introduced at a flow rate of 77.1 sccm, 18.6 sccm, and 14.3 sccm, respectively. In the 540.34 GHz to 540.40 GHz spectral window of Fig. 2, transitions from CF$_2$O and CF$_2$ are observed in the initial trace, while in the 607.60 GHz to 607.62 GHz spectral window of Fig. 3, transitions from SiO and CF$_2$O are observed. The transitions from CF$_2$O are unidentified; the CF$_2$ transition is assigned as $18_{2,17} - 17_{1,16}$ while the SiO transition is assigned as $J = 14 - 13$.

Number densities of 1.0×10^{13} cm^{-3} and 4.7×10^{11} cm^{-3} are derived for CF$_2$O and CF$_2$ during photoresist etching (bottom trace) in Fig. 2. Number densities of 2.0×10^{13} cm^{-3} and 5.7×10^7 cm^{-3} are derived for CF$_2$O and SiO during SiO$_2$ etching (bottom trace) in Fig. 4. The plasma is assumed to have a uniform rotational temperature of $T = 300$ K, although experimental studies suggest slightly higher temperatures (300 K to 450 K) with some spatial nonuniformity [6-10].

During the cleaning process, the concentrations of cleaning byproducts (SiO, CF$_2$O, and CF$_2$) decrease and effectively vanish below our detection limits as fluorocarbon and silicon dioxide deposits are removed from the chamber wall and internal components. Simultaneous with this decrease, the signal strength of the O$_3$ rotational line ($11_{5,7} - 12_{4,8}$) in Fig. 2 near 540.3 GHz gains in strength, indicating a significant buildup of O$_3$ in the reactor, reaching a peak of 1.3×10^{12} cm^{-3}. The observation that the ozone level increases with chamber cleanliness is consistent with the depletion of carbon-containing deposits which are highly reactive with the O$_3$. Because the ozone is associated with a cleaned reactor, it should be present regardless of the initial type of wall and surface contamination. The increase of ozone signal strength and the decrease of CF$_2$O, CF$_2$, and SiO signal strengths can thus be used to assess the progress of removing residues deposited during the previous plasma etching process.

Etch Endpoint Detection

The detection sensitivity of 2×10^7 cm^{-3} demonstrated in the previous section for SiO
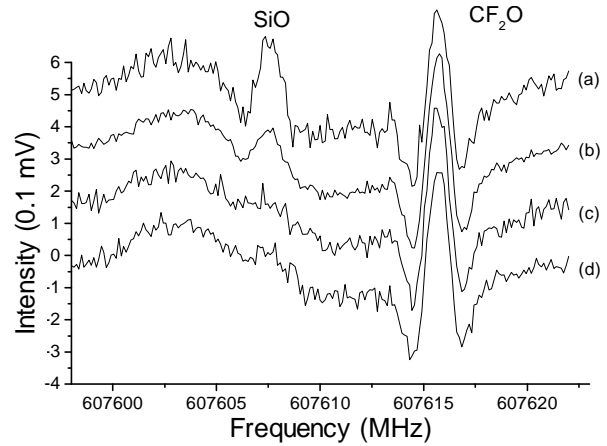

FIGURE 4. Spectra observed during the etching of a SiO$_2$ layer (approximately 500 nm thick) on a Si wafer using a plasma formed by flowing 14.3 sccm, 7.2 sccm, and 88.5 sccm of octafluorocyclobutane (c-C$_4$F$_8$), O$_2$, and Ar, respectively, at a chamber pressure of 6.7 Pa and showing the $J = 14 - 13$ transition of SiO and an unassigned transition of CF$_2$O, also present in a pure CF$_2$O and N$_2$ mixture. Trace (a) shows the intensities of SiO and CF$_2$O at the beginning of the etching of SiO$_2$ and was obtained by sweeping the BWO twice over the two lines over a total time interval of approximately 1 min. The concentrations of SiO and CF$_2$O at this stage are approximately 9.2×10^{14} cm^{-3} and 1.0×10^{14} cm^{-3}, respectively. Trace (b) corresponds to the average of 7 spectral traces over the same frequency interval and was initiated immediately after trace (a) and lasted for a period of approximately 4 min. The trace was acquired to look for evidence of the decrease of SiO. Trace (c) was acquired immediately after trace (b) and was finished approximately 7 min into the etching process and shows that the SiO has nearly vanished due to complete etching of the SiO$_2$ from the wafer. Trace (d) was acquired 4 min later and shows the SiO concentration remains suppressed from the initial value.

suggests the possibility of using the concentration of SiO to assess the progress of an etch process. A number of other techniques have been studied for etch endpoint detection, as reviewed by Sun *et al.* [11], including their tunable diode-laser method. Here, we use SiO measurements to monitor the fluorocarbon plasma etching of a thermally grown SiO$_2$ layer about 500 nm thick on a Si wafer. In Fig. 4 we show the signal strengths of SiO and CF$_2$O transitions near 607 GHz at several stages of the etching by an octafluorocyclobutane (c-C$_4$F$_8$), O$_2$, and Ar plasma, at flow rates of 14.3 sccm, 7.2 sccm, and 88.5 sccm, respectively, and a total chamber pressure of 6.7 Pa (50 mTorr). The top trace (a) of approximately 1 minute duration corresponds to two averaged frequency sweeps of the BWO and was acquired at the beginning of the etch process. The initial number densities obtained for SiO and CF$_2$O under the present conditions are 9.2×10^{14} cm^{-3} and

1.0×10^{14} cm^{-3}, respectively, again assuming a mean reactor gas temperature of 300 K. The second trace (b) of approximately 4 minute duration was acquired immediately after the first trace and corresponds to 7 averaged sweeps of the BWO. Here, the BWO was continually swept over the spectral window until the SiO signal amplitude was significantly decreased. The third trace (c) was acquired approximately 7 minutes after the start of the etching process and clearly shows the near total extinction of the SiO signal, whereas the CF$_2$O concentration is constant. This significant decrease of the SiO signal intensity was a result of complete removal of the SiO$_2$ layer on the wafer. As seen in the bottom trace (d) in Fig. 5, a residual SiO signal level remains 4 minutes after the SiO$_2$ layer had been removed and the underlying crystalline silicon wafer was exposed to the plasma. The low O$_2$/C$_4$F$_8$ ratio in this recipe favored etching of SiO$_2$ over crystalline silicon. The much lower etch rate of underlying crystalline silicon resulted in the decrease of the SiO signal to a significantly lower residual level once the SiO$_2$ layer was completely removed. Of course, to obtain a more reasonable time resolution (< 0.5 s) in the present study it would be preferable to fix the BWO frequency to the SiO absorption frequency and monitor the signal strength of the SiO transition as a function of time. Such a measurement is straightforward to implement, as the BWO is frequency stabilized and thus easily fixed to a specific frequency.

As with many other etch endpoint detection techniques, the present sensitivity is not sufficient to detect endpoints when the ratio of the etched area to the total wafer area is small (i.e., low open area ratio). The present detection sensitivity, however, is useful for detecting the endpoint of removing large areas of silicon-containing films from the inside of a processing chamber. One example of such application is the endpoint detection in cleaning chemical vapor deposition (CVD) chambers. This technique is particularly valuable for endpoint detection in remote plasma downstream chamber cleaning since traditional optical emission spectroscopy (OES) based endpoint detection is no longer viable due to the lack of an excitation source of the etching byproducts in the downstream chamber. Moreover, improvements in sensitivity are possible with multipass schemes based on resonant or nonresonant cavities, potentially allowing the monitoring of endpoints for etch processes with a low open area ratio.

CONCLUSION

In the present paper we described a new and sensitive method for the detection and quantification of chemical species in low pressure (< 133 Pa {1 Torr}) plasma reactors. The technique provides the ability to monitor a plethora of molecular species, as nearly all the critical chemical components of semiconductor plasmas have submillimeter wavelength spectra. Although not yet demonstrated to high accuracy, the technique offers the potential to provide quantitative information on the number densities of a variety of chemical species in the reactor, not available by other methods. Future efforts will be directed at developing the submillimeter method into an accurate tool for the quantification and monitoring of chemical species in semiconductor processing plasmas

REFERENCES

1. Krupnov, A.F. and O.P. Pavlovsky, *Int. J. Infrared Milli.* **15,** 1611 (1994).
2. Krupnov, A.F., *Int. J. Infrared Milli.* **22,** 1 (2001).
3. Hargis, P.J., Jr., et al., *Rev. Sci. Instrum.* **65**, 140-154 (1994).
4. Olthoff, J.K. and K.E. Greenberg, *J. of Res. of the Natl. Inst. of Stand. and Technol.* **100**, 327-339 (1995).
5. Tison, S.A. and J.P. Looney, *J. Res. Natl. Inst. Stand. Technol.* **100**, 75 (1995).
6. Haverlag, M., F.J.d. Hoog, and G.M.W. Kroesen, *J. Vac. Sci. Technol. A* **9**, 327 (1991).
7. Haverlag, M., et al., *J. Vac. Sci. Technol. A* **14**, 380 (1996).
8. Booth, J.P., G. Hancock, and N.D. Perry, *Appl. Phys. Lett.* **50**, 318 (1987).
9. Booth, J.P., et al., *Plasma Sources Sci. Technol.* **7,** 423 (1998).
10. Steffens, K.L., *unpublished results*.
11. Sun, H.C., et al., *Appl. Phys. Lett.* **64**, 2779 (1994).